Excitable calcium wave propagation in the presence of localized stores

C. S. Pencea and H. G. E. Hentschel
Department of Physics, Emory University, Atlanta, Georgia 30322
(Received 2 May 2000)

We study the propagation of calcium waves in the presence of a discrete distribution of calcium stores. Calcium-induced calcium release coupled to diffusion can be used to produce a criterion for wave propagation across connected clusters of stores. The velocity of the resulting wave and its relationship to the frequency of the excitatory stimulus can then be described using percolation theory. Simulations show a homogenous and a fractal regime and are in agreement with both experiments and theory.

PACS number(s): 87.18.Pj, 87.16.Yc, 87.16.Ac

I. INTRODUCTION

Recently there has been considerable interest in the spatiotemporal dynamics of calcium inside cells. Calcium is known to affect a variety of cell processes, from fertilization and proliferation, to the death of the cell [1]. In neurons calcium influences the information processing of neuronal signals, as well as long-term potentiation, the underlying mechanism believed to be responsible for short-term memory [2].

Calcium oscillations can be triggered by chemical, electrical, or even mechanical stimuli. Stores or pools of calcium exist inside the cell and under certain conditions calcium can be released, producing an increase of free cytosolic calcium, which contributes to calcium oscillations and propagation. This is due to the free calcium itself triggering the release of stored calcium if it reaches a critical concentration—a phenomenon known as calcium-induced calcium release (CICR).

The diffusion of calcium is crucial in transforming these temporal calcium oscillations into spatial calcium waves, and they show many similarities to the excitable chemical waves [3], though the nonlinear mechanisms involved are different: the increasing cytosolic calcium concentration does not trigger a chemical reaction but the release of calcium from the filled stores interacting with the cytosolic calcium wave front.

The stored calcium can be studied from several viewpoints. Taking a macroscopic point of view, one can define a smooth local concentration of stored calcium [4–7] whose temporal and spatial variation can be described by a partial differential equation. Such an approach may model the endoplasmic reticulum smoothly filling a cytosolic domain and the local release of stored calcium at a rate k coupled to diffusion D can lead to waves travelling with velocities $v \sim \sqrt{Dk}$ [6]. But what happens when the stores are well separated and the release time for the calcium $\tau \sim 1/k$ is much shorter than the propagation time $\tau_{prop} \sim r^2/D$ between stores, where r is a typical distance between discrete stores? In this case the stores will begin to act as nodes in a circuit and new phenomena can be expected to appear. In addition to the existence of such spatial inhomogeneities, which act as sources of quenched disorder on the dynamics, noise in the form of thermal fluctuations may significantly affect the propagation of calcium waves in cells.

In this paper we study the dynamics of calcium wave propagation in the presence of such localized calcium pools with CICR coupled to extended diffusive mechanisms for the free calcium dynamics.

In Sec. II we derive the conditions for calcium wave propagation and more particularly an equation for the velocity of the calcium wave. We show how the discrete distribution of the stored calcium affects this propagation. We use percolation theory to derive scaling estimates for the velocity of the excitable calcium using the observation that close similarities exist to the mechanisms controlling the spread of forest fires and the spatial transmission of infections in disordered media. We also study how the frequency of stimulation changes the velocity of the wave (dispersion), and the cutoff frequency at which the wave does not propagate any more. These pieces of information are necessary in order to understand how and what type of signals can be transmitted inside a living cell by CICR.

Finally in Sec. III we show simulations based on our model. They show clearly a fractal and a homogenous regime of the calcium signal propagation, depending on the density of stores and on the amount of stored calcium. The simulations are similar to experimental results that are explained by theory.

II. THEORY

Calcium transport between stores and the cytosol has been investigated by several groups [4,8–13], who have identified the net calcium flux from a store as due to three major mechanisms:

$$J = J_{CICR}(c,c_s) + J_{leak}(c_s) + J_{refill}(c) = V_{CICR}\frac{c_s^m}{c_s^m + K_s^m}\frac{c^n}{c^n + K_c^n} + Kc_s - V_{refill}\frac{c^p}{c^p + K_{refill}^p}, \tag{1}$$

where c and c_s represent the concentration of calcium ions in the cytosol and stored in the pools, respectively. Equation (1) has been used both for compartmented models and for the case in which the stored and cytosolic calcium concentrations are treated in a continuous fashion. In the latter case c and c_s are calculated by averaging, respectively, the number of free and stored calcium ions over a volume that in-

cludes many stores. In the right-hand side of Eq. (1) the first term describes CICR, with K_c and K_s representing the threshold concentrations of calcium, in the cytosol and in the stores, respectively, needed for CICR to occur, while V_{CICR} is the maximum rate of calcium release, which is obtained when the both c and c_s are much greater than their corresponding threshold values. The second term represents a linear leak from the stores into the cytosol and is necessary to ensure the stability of the store-cytosol system. The last term represents the active refill of the stores, V_{refill} and K_{refill} being the maximum refill rate and the threshold concentration of cytosolic calcium at which the refill starts, respectively. The Michaelis-Menten form of these fluxes, where the Hill coefficients m, n, and p are positive integers representing the cooperativity of the kinetics involved, should be valid provided we are interested in processes at timescales that are large compared to the molecular timescales describing the receptor-ligand dynamics.

Several variations of the CICR dynamics described above have been investigated. As CICR may be inhibited at very high concentrations of cytosolic calcium, Bezprozvanny, Ehrlich and Watras [14,15] have modified Eq. (1) to describe this aspect of the calcium dynamics. More complex models in which the dynamics of the second messenger inositol trisphosphate (IP_3) [16–18] is coupled to that of calcium have also been considered. The essential features in Eq. (1)—specifically excitability and calcium oscillations—are, however, also present in these models and in this paper we will use Eq. (1) as our starting point for investigating the effect of spatial localization of stores on calcium propagation.

Here we study the manner in which the distribution and properties of a set of discrete stores affects the propagation of calcium signals. For a given distribution of stores, the concentration of free calcium ions obeys the diffusion equation

$$\frac{\partial c(\mathbf{r},t)}{\partial t} = D\nabla^2 c(\mathbf{r},t), \tag{2}$$

with the stores acting as point sources. D is the effective diffusion coefficient that in general includes buffering of the cytosolic calcium. The number $n_i(t)$ of calcium ions inside the store i located at position $\mathbf{r}_i$ is given by

$$\frac{\mathrm{d}n_i(t)}{\mathrm{d}t} = g[n_i(t), c(\mathbf{r}_i,t)]. \tag{3}$$

The function g describes the integrated flux of calcium between the store and the cytosol (CICR, refill, leak); an analytical expression for g can be obtained from Eq. (1) observing that $c_s = n_i N_s$, where N_s is the local volume density of stores.

In the absence of boundaries the coupled system formed by Eqs. (2) and (3) can be formally solved:

$$c(\mathbf{r},t) = c_0(\mathbf{r}) + \sum_i \int_0^t d\theta \, \frac{g[n_i(\theta), c(\mathbf{r},\theta)]}{[4\pi d D(t-\theta)]^{d/2}} \exp\left(\frac{-(\mathbf{r}-\mathbf{r}_i)^2}{4dD(t-\theta)}\right),$$

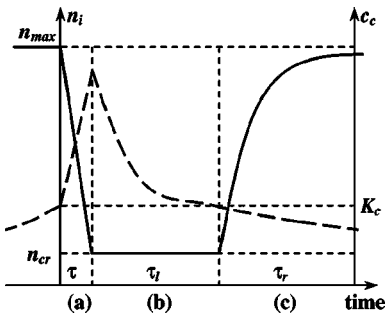

FIG. 1. Simplified excitable dynamics of the store. Continuous line: amount of stored calcium; dashed line: local concentration of cytosolic calcium near a discrete store. (a) Constant rate CICR. The CICR and refill mechanisms are both activated, but CICR dominates. (b) Latent interval. The CICR and refill mechanisms are both activated, they cancel each other, an increased local concentration of cytosolic calcium exists until diffusion disperses it. (c) Refill phase. The CICR mechanism is inactive. The amount of stored calcium relaxes exponentially towards the equilibrium value dictated by the leak and refill mechanisms. The store is excitable again. The characteristic time scales τ, τ_l, and τ_r are estimated in text.

$$n_i(t) = n_i^0 + \int_0^t d\theta \, g[n_i(\theta), c(\mathbf{r}_i,\theta)], \tag{4}$$

where $c_0(\mathbf{r})$ and n_i^0 are the, respective, initial values and d is the dimensionality of the domain.

Though general, the solution above is fairly intractable due to the coupling between $c_s(\mathbf{r}_i,t)$ and $n_i(t)$, described by g. Using a less complicated, yet biologically intuitive model for the store, one can obtain a function g simpler than the one described by Eq. (1), and thus a piecewise uncoupled, integrable system in Eq. (4). Such a form is sufficient for our purposes as our interest lies in determining if and when a specific store is involved in CICR as a result of a given initial stimulus. In this manner we obtain an alternate description of the wave propagation, more useful in constructing chemical networks.

Essentially each store can be at any instant in one of the following three states (see Fig. 1): (a) the CICR state: if $c > K_c$ and $n_i > n_{cr} \equiv K_s/N_s$, CICR dominates and the store releases at a constant rate $g = V_{CICR}/N_s$; (b) the latent state: if $n_i \lesssim n_{cr}$ and $c > K_c$, CICR is no longer dominant, but only balances the refill mechanism, thus $g \approx 0$; (c) the refill state: if $K_{refill} < c < K_c$ the refill dominates as CICR is inactivated, the leak and refill will eventually balance the refill as $n_i \to n_{max}$ (n_{max} is the maximum number of calcium ions that the store can hold), in this state $g = -V_{refill}/N_s + K n_i$. The function g obtained from this three-state model corresponds to the high cooperativity limit of the CICR and refill mechanisms, obtained for large Hill coefficients ($m,n,p \gg 1$).

Figure 1 shows the excitable behavior of the stored calcium and of the cytosolic calcium near the store as a result of an external excitation (local stimulus or increase of the cytosolic calcium): a store in the refill state changes its state to the CICR state as c reaches K_c, then to the latent state as n_i drops under n_{cr}, then back again to the refill state as c falls under K_c.

There are three time scales, τ, τ_l, and τ_r associated with the CICR, latent, and refill states, respectively. The time τ

can be estimated from the period during which CICR is dominant, τ_l describes how long the store stays in the latent state, and τ_r approximates the time necessary for the pool to refill completely. Estimates of these three time scales are

$$\tau \sim \frac{n_{i,0}N_s}{V_{CICR}}; \quad \tau_l \sim \frac{1}{D}\left(\frac{n_{i,0}}{K_c}\right)^{2/d}; \quad \tau_r \sim \frac{1}{K}, \tag{5}$$

where $n_{i,0}$ represents the number of stored calcium ions at the moment when the stimulation occurs (beginning of CICR). In general $n_{i,0}$ depends on the recent history of the store (i.e., how long the store has been in the refill state before the stimulation event) and can differ between successive excitations; for stores that have been in the refill state for a long time $n_{i,0} \approx n_{max}$. The estimate for τ_l can be obtained from the condition that the released calcium is spread by diffusion until the calcium concentration near the store drops under the threshold K_c.

Based on this model of the store dynamics we can obtain a criterion as to whether propagation between a pair of stores results in the second store being triggered into the CICR state. We can regard the wave as an avalanche of such elementary propagations between nearby stores.

Thus the release of calcium by pool i starts at $t=0$ and stops at $t=\tau$. This cytosolic calcium diffuses away and at any time $t>\tau$ the free calcium concentration at store j located at $\mathbf{r}_j$ will be observed to increase by an amount

$$\Delta c(r,t) = \frac{n_{i,0}}{\tau}\int_0^\tau d\theta [4\pi dD(t-\theta)]^{-d/2} \exp\left(\frac{-r^2}{4dD(t-\theta)}\right)$$

$$= \frac{n_{i,0}}{r^d}\langle F(u)\rangle_{[u_{t-\tau},u_t]}, \tag{6}$$

where $t>\tau$, $r \equiv |\mathbf{r}_j - \mathbf{r}_i|$, $u_t \equiv 4dDt/r^2$, and $F(u) \equiv (\pi u)^{-d/2}\exp(-1/u)$. Here we introduced the notation

$$\langle F(u)\rangle_{[u_1,u_2]} \equiv \frac{1}{u_2-u_1}\int_{u_1}^{u_2} du\, F(u) \tag{7}$$

to mean an average over the interval in square brackets. The propagation criterion requires $\Delta c(\mathbf{r},t)$ to become greater than the CICR threshold K_c at some time t, or using Eq. (6)

$$\max_t \langle F(u)\rangle_{[u_{t-\tau},u_t]} \geqslant \frac{K_c r^d}{n_{i,0}}. \tag{8}$$

This criterion considers only the most important term in the sum in Eq. (4), thus neglecting the possible combined effect of several releasing stores. Note that far enough from the source the average is over a small interval, reaching the limit for instantaneous release as $r \to \infty$.

As $F(u)$ reaches its maximum value for $u=2/d$, in the limit $u_\tau \ll 1$ the maximum value of the average of $F(u)$ in Eq. (8) is obtained if the average is taken over the interval $[2/d-u_\tau/2, 2/d+u_\tau/2]$. Thus to the lowest order in τ

$$\frac{n_{i,0}}{r^d K_c} \geqslant \left(\frac{2\pi e}{d}\right)^{d/2}\left(1-\frac{d^5D^2\tau^2}{4r^4}\right)^{-1}. \tag{9}$$

The propagation condition above becomes more stringent as τ increases, or as the CICR rate decreases [see Eq. (5)].

From this point on we will consider only the instantaneous release limit case ($\tau=0$). The equality in Eq. (9) defines the minimum amount of calcium, whose release will result in an excitation of site j

$$n_{i,min} = \left(\frac{2\pi e}{d}\right)^{d/2} r^d K_c, \tag{10}$$

and also the range of store i, which is the maximum distance at which the release at store i will trigger other stores to release:

$$r_{max} = \left(\frac{d}{2\pi e}\right)^{1/2}\left(\frac{n_i}{K_c}\right)^{1/d}. \tag{11}$$

Now consider consecutive stimulations of site i and let us analyze the response of site j as a function of the time period between two successive stimuli. We assume that the signal propagates at least when the site i is completely filled ($n_{i,0} \to n_{max}$), or in other words that n_{max} satisfies the propagation criterion for the pair of stores considered. In the opposite case the stimulus will never propagate to site j. A second stimulus at site i will be transmitted to site j only if the site i has been filled with at least $n_{i,min}$ calcium ions. This occurs only after a minimal time interval

$$t_{min} = \tau_l + \frac{n_{i,min}N_s}{V_{refill}} \tag{12}$$

between the two stimuli, with τ_l estimated from Eq. (5). Interestingly, t_{min} depends not only on the store distribution and properties, but also on the recent history represented by the amount of calcium released by the first stimulus $n_{i,0}$.

In the limit of low stimulus frequency ($f \ll t_{min}^{-1}$), the pool i is filled completely when each stimulation occurs, and each stimulus results in propagation to site j. In the opposite limit (high frequency, $f \gg t_{min}^{-1}$), pool i never spends enough time in the refill state, and accordingly no stimulus will propagate to site j.

The maximum frequency at which consecutive stimuli can result in propagations of the excitation between the two pools can be estimated as t_{min}^{-1}, with $n_{i,0}=n_{i,min}$. This is the case when the stimulation at site i occurs always exactly when $n_{i,0}=n_{i,min}$. The amount of calcium in the store i at the moment when the stimulation occurs can be calculated as a function of the amount released by the previous stimulus. The resulting discrete map has a fixed point for a low frequency of the stimulus, and shows one period doubling bifurcation at $f \sim t_{min}^{-1}$, when the fixed point becomes unstable. The period two solution corresponds to the case when consecutive stimuli find the store i filled with different amounts of calcium, one higher and the other lower than the fixed point value. After the release of the higher amount of calcium the store i has to spend more time in the latent state before entering the refill state. The lower time spent in the refill state before the next stimulation allows the store to refill only up to the minimum value of the period two (stable) solution. After the next stimulus the store spends less time in the latent state, and thus more time in the refill state, refilling

up to the higher value and so on. If the distance between the stores i and j is chosen appropriately, $n_{i,min}$ can be tuned [see Eq. (10)] between the minimum and the maximum values of the discrete map's period two solution. In such excitation period, doubling at the receiver store j will occur, as only every other stimulus at site i results in propagation to site j.

Now we note that there exists a relationship between calcium wave propagation across a set of discrete stores and percolation. Given a distribution of stores, we can add formally a bond between each pair of stores that meets the propagation criterion (9). Thus we obtain connected clusters of stores; once the external stimulus triggers one store inside a cluster, the excitation will propagate as an avalanche to all the other stores that belong to it. If a is the typical length of a bond the characteristic time for the excitation to propagate across it is given by

$$t_0 \sim \frac{a^2}{D}. \tag{13}$$

The average number of stores that exist in a volume r_{max}^d is $p = N_s r_{max}^d$, a dimensionless parameter that summarizes all percolation-related properties of the store distribution. In the limit $p \ll 1$ there are very few bonds and only very small clusters exist. This case is of no interest since no signal can propagate. The opposite limit $p \gg 1$ corresponds to the continuous limit, with typical distances between stores much smaller than the range r_{max}. This situation is described properly by a system of partial differential equations.

Here we will investigate the intermediate case $p \sim 1$. It can be argued that in this case $a \sim r_{max}$. If p is greater than the percolation threshold p_c an infinite cluster of connected stores exists. Let us consider a stimulus that triggers one of its stores into the CICR state. The propagating wave will behave differently at early times as opposed to late times. At early times the fractal regime is observed. The average distance to the firing stores (measured from the initially triggered site) scales with time as

$$R \sim a\left(\frac{t}{t_0}\right)^{\tilde{\nu}} \sim \xi\left(\frac{t}{t_\xi}\right)^{\tilde{\nu}}, \tag{14}$$

where ξ is the correlation length, t_ξ is the characteristic time needed by the signal to propagate to a distance on the order of ξ ($R \sim \xi$ at $t = t_\xi$), and $\tilde{\nu}$ is the graph dimension of the percolating cluster [19]. The exponent $\tilde{\nu}$ is 0.885 for $d=2$ and 0.735 for $d=3$. We remark that in both cases $\tilde{\nu} < 1$, thus in the fractal regime R increases slower than linearly with the time t. The fractal regime is observed as long as $R \ll \xi$ or $t \ll t_\xi$.

At late times $t \gg t_\xi$ (or $R \gg \xi$) the homogenous regime is observed. In this regime one expects R and t to be proportional:

$$R \sim \xi \frac{t}{t_\xi}. \tag{15}$$

The Eqs. (14) and (15) can be combined into the scaling form

$$R \sim a\left(\frac{t}{t_0}\right)^{\tilde{\nu}} h\left(\frac{t}{t_\xi}\right), \tag{16}$$

where the function h describes the crossover between the two regimes. From the behavior in the fractal regime $h(x) \sim h_0$ for $x \ll 1$. To obtain the correct exponent of t for the homogenous regime one needs $h(x) \sim x^{1-\tilde{\nu}}$ for $x \gg 1$.

In the homogenous regime the wave front travels at a constant velocity that can be estimated as

$$v \sim \frac{a}{t_0}\left(\frac{\xi}{a}\right)^{1-1/\tilde{\nu}} \sim \frac{D}{a}\left(\frac{|p-p_c|}{p_c}\right)^{(1/\tilde{\nu}-1)\nu}. \tag{17}$$

Here ν is the exponent that relates the correlation length to the difference from the percolation threshold p_c:

$$\frac{\xi}{a} \sim \left(\frac{|p-p_c|}{p_c}\right)^{-\nu}. \tag{18}$$

In the presence of discrete stores the velocity is proportional to the diffusion coefficient D, in contrast with the case of a continuous distribution of stores.

If the store triggered initially belongs to a finite cluster the wave will die out once it reaches all the sites of the connected cluster. As a consequence, below the percolation threshold only the fractal regime is observed.

Let us now investigate how the velocity of the wave front depends on the frequency of the stimulus. At low frequencies the refill between successive stimuli is complete ($n_{i,0} \approx n_{max}$) and all wave fronts are identical (assuming that the initial conditions set by consecutive stimuli are the same). Between consecutive stimuli the stores enter the refill state, the amount of stored calcium grows and thus bonds between pairs of stores are added, forming small connected clusters. As more bonds are added the clusters grow and coalesce and once the percolation threshold is reached, the correlation length starts decreasing from the theoretically infinite value at the percolation threshold towards the finite, presumably small value that corresponds to completely filled stores. As the frequency increases the time spent in the refill state gets lower than τ_r and the correlation length at the moment when the stimulations occur gets larger. Thus, because the exponent of ξ in Eq. (17) is negative, the velocity decreases with frequency in the homogenous regime. As the frequency increases further and fewer links have enough time to grow, we approach the percolation critical concentration of bonds (from above) and the diverging correlation length ξ gets bigger than the size of the domain considered. The crossover from the homogenous to the fractal regime is observed. Finally more links are broken at an even higher frequency, and the wave does not propagate any more, as the grown cluster of sites falls under the percolation threshold.

III. SIMULATION RESULTS

To simulate the propagation of the excitation wave, identical stores of calcium were placed randomly inside a square domain. All the stores are initially filled with the same amount of releasable calcium, n_{max}. While n_{max} has been changed between different simulations, all the other parameters were kept fixed. The simulation is started by triggering

a store, located close to the center of the domain, into the CICR state. The current release will cause the stores located within a distance smaller than r_{max} to release also. The times when the new releases will occur are calculated numerically, generating a list of future events and their corresponding times. The site that releases next is determined by analyzing the list and the clock is advanced up to its release time. The release by the new site adds new elements in the list, and the process is repeated while the event list is not empty. All the sites that release enter the latent state. The moment when the latent state ends and the refill state starts is calculated and this new event is also added to the list.

At high stored calcium concentration the correlation length ξ is much smaller than the size of the domain and the homogenous regime is observed. Snapshots of such a typical evolution are presented in Fig. 2. After a short transient time, the wavefront approximates a circle that expands with roughly constant radial velocity. For a smaller amount of stored calcium the correlation length ξ gets bigger than the size of the domain, as the store distribution gets closer to the percolation threshold, and the fractal regime is observed (Fig. 3). The wavefront is very irregular and consists of puffs of calcium release that propagate along individualized branches of the connected cluster. The traveling puffs split if the branch has a bifurcation and die when they reach the end of a branch.

The difference between the two typical patterns shown in Figs. 2 and 3 is illustrated in a more quantitative manner in Fig. 4, where the distance from the origin of the excitation is plotted as a function of the time when the excitation occurs at the respective store. Figure 4(a) corresponds to the homogenous regime presented in Fig. 2, with the distance to the firing sites increasing linearly with the time when they fire. On the other hand, in the fractal regime shown in Fig. 3 two puffs that have just separated from each other will not propagate in general towards the radial direction, moreover they may even move back towards the origin. As a result [see Fig. 4(b)] the corresponding graph will show individualized branches that correspond to different travelling puffs. The fractal nature of the graph in Fig. 4(b) is reflected in the nonlinearity between the linear and chemical distances, and ultimately in the graph dimension $\tilde{\nu}$ [see Eq. (14)]. The velocity at which the excitation propagates between two given stores has also been measured as a function of n_{max}. The two stores were chosen so that they are well inside the domain (to avoid finite-size effects), but also far enough from each other. Then an excitation wave was started by setting one of the two stores in the CICR state. The velocity was measured by recording the time when the second site fires. Figure 5 shows how the velocity increases with the amount of releasable calcium. Plateaus of almost constant wave velocity are separated by discontinuities. The discontinuities reflect the opening of a shorter path as a result of an increased connectivity when r_{max} increases. The velocity increases slightly inside the plateaus, because a higher amount of releasable calcium translates into a slightly shorter propagation time t_0 across each bond. This dependence is very weak and has been neglected in Eq. (13), however it has been taken care of numerically. A similar pattern change is also seen in fluorescence imaging experiments done on Xenopus oocytes injected with IP_3. At high concentration of IP_3 regular circular waves similar to those in Fig. 2 are observed, while if less IP_3 is injected, individualized peaks of free calcium concentration travel through the cytosol, resembling the simulation in Fig. 3. IP_3 enhances the release of calcium from stores by binding to specific sites and thus activating the calcium release channels [12]. An increased IP_3 concentration will increase the number of active stores, i.e., stores that can release calcium by CICR and thus contribute to the propagation of the calcium signal. Since all stores considered in our simulations are active the net effect of adding more IP_3 is to modify the store distribution by adding more stores. As N_s increases the percolation parameter p increases also, which above the percolation threshold leads to a decrease of the correlation length ξ. In our simulations we produced the same effect by modifying n_{max}, which in our algorithm is equivalent to modifying N_s. The similarity between the pattern change seen experimentally and in the simulation is a strong argument that the propagation of calcium signals is related to percolation.

The same IP_3-controlled qualitative behavior has been shown also in simulations performed by Bugrim *et al.* [18], which have considered a model with discrete stores of finite volume and have solved numerically the partial-differential equation system that describes the calcium dynamics. Bugrim *et al.* [18] have shown the existence of a critical IP_3 concentration under which the calcium wave does not propagate. The average propagation distance of abortive waves diverges according to a power low near the critical concentration of IP_3:

$$R_p \sim ([IP_3]_{crit} - [IP_3])^{-a}. \tag{19}$$

Since $[IP_3]_{crit}$ corresponds to the percolation threshold p_c and, as discussed above, p increases with the concentration of IP_3, the equation above should have the same exponent as the correlation length in Ref. [18]. Bugrim *et al.* obtained from simulations $a \approx 1.74$, while the expected theoretical value for ν is 4/3.

The critical concentration of IP_3 can be estimated from the condition that the concentration of stores activated by IP_3 equals the percolation threshold, or $p_{active} = p_c$ at $[IP_3] = [IP_3]_{crit}$. One can assume a typical Michaelis-Menten activation by IP_3, namely,

$$p_{active} = p_{total} \frac{[IP_3]}{[IP_3] + [IP_3]_0}, \tag{20}$$

where p_{total} is the total concentration of stores, of which p_{active} are activated by IP_3, and $[IP_3]_0$ is the threshold activation concentration (the concentration at which half of all stores are activated by IP_3). Thus the relation between the critical IP_3 concentration and the total concentration of stores is

$$[IP_3]_{crit} = \frac{p_c [IP_3]_0}{p_{total} - p_c}, \tag{21}$$

again in qualitative agreement with the results of Bugrim *et al.* [18].

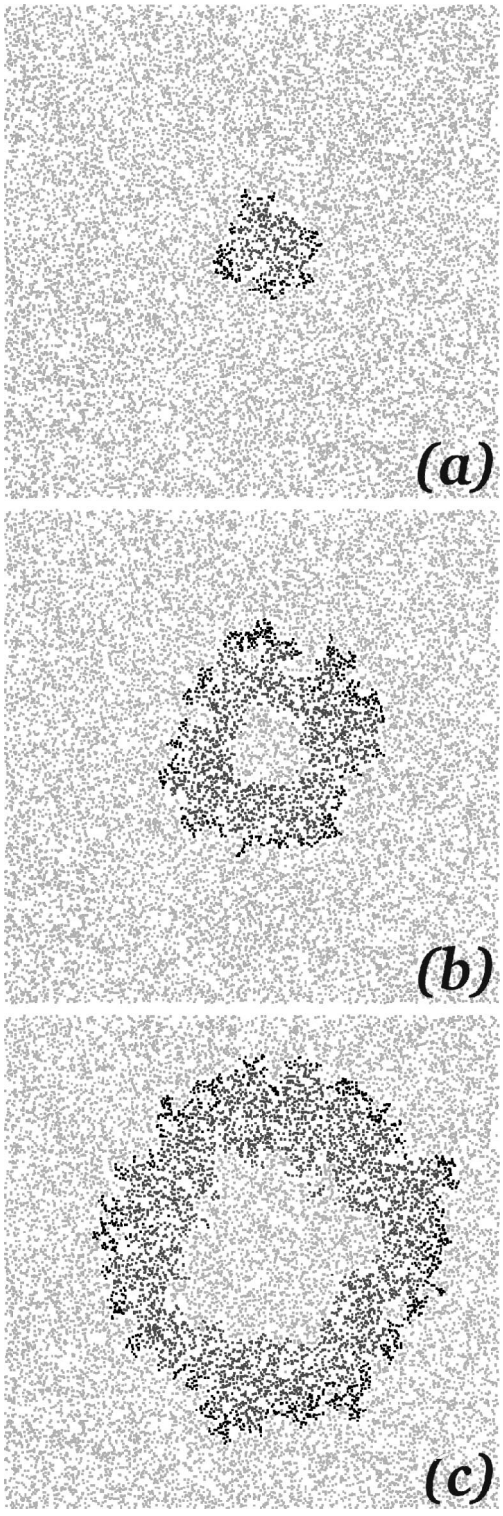

FIG. 2. Formation of a circular wave in the homogenous regime. The wave is started by exciting one central store at $t=0$. Initially all the stores are filled with the maximum amount of calcium, n_{max}. The stores that have fired in the last 0.5 s are colored in black. Light gray is used to describe the excitable sites (in the refill state) and dark gray to describe the latent sites. Parameters used: size of the domain: 240 μm; number of stores: 16 396; $n_{max}/K_c = 66.7\ \mu\text{m}^2$ (or $p=2.22$); $V_{refill}/n_{max}=10\ \text{s}^{-1}$; $D=10.0\ \mu\text{m}^2/\text{s}$. The images (a)–(c) are snapshots taken at equal time intervals of 2 s after the initial excitation in the center. (a) transient irregular front; (b),(c) circular fronts propagating with constant radial velocity.

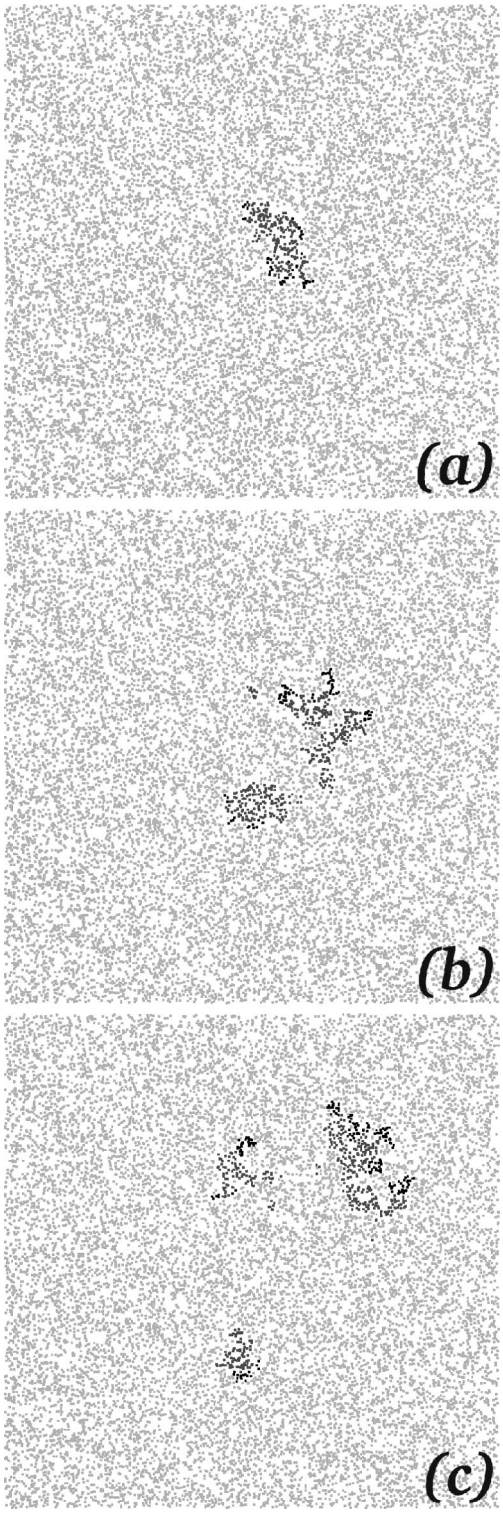

FIG. 3. The fractal regime: irregular wavefront that persists up to the size of the domain. The parameters are as in Fig. 2, except $n_{max}/K_c=42.7\ \mu\text{m}^2$ (or $p=1.42$) and $V_{refill}/n_{max}=15.625\ \text{s}^{-1}$.

IV. CONCLUSIONS

In this paper excitable CICR in the presence of localized stores has been considered. Simulations for different amounts of releasable calcium show clearly a fractal regime for low stored calcium and a homogenous regime for high stored calcium concentrations, as percolation theory predicts. The similarity with experimental results strongly suggest that

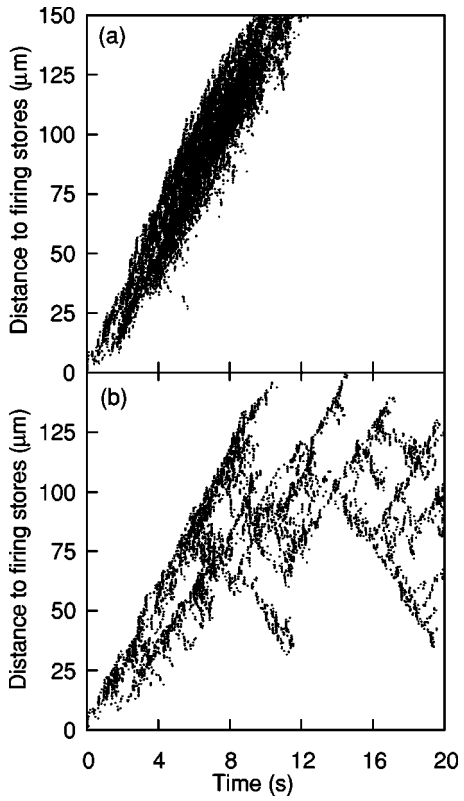

FIG. 4. Propagation of the wave front: (a) the homogenous regime; (b) the fractal regime.

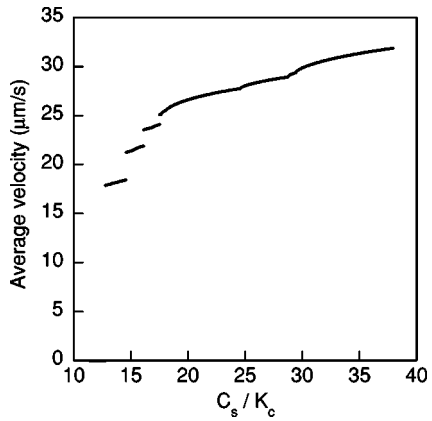

FIG. 5. Velocity dependence on stored calcium. Other parameters as in Fig. 2.

percolation related aspects are very important in understanding the propagation of calcium signals.

Our results suggest a plausible mechanism for frequency encoded calcium signaling. The time interval between consecutive signals controls the amount of calcium available for the new release, and thus the connected cluster across which the signal will propagate. A high frequency translates into a smaller region in which the calcium signal can propagate. The resulting signaling mechanism becomes very powerful if instead of a single stimulation one considers the effect of two or more stimuli that occur in different regions of the cell. A biologically plausible distribution may have the stores organized in calcium circuits—well-defined paths of connected stores forming ''wires'' that transmit the calcium signals between different regions of the cell. The nodes of such a circuit can play an important role in analyzing calcium signals since this is where different signals interact. We will show in a following paper how specific distributions of stores in the vicinity of a node can perform coincidence detection and elementary logical operations on calcium signals.

ACKNOWLEDGMENTS

We would like to thank Criss Hartzell, Fereydoon Family, and Stefan Boettcher. This work was supported by a Collaborative Research Grant from NATO.

[1] M. Berridge, M. Bootman, and P. Lipp, Nature (London) **395**, 645 (1998).
[2] T. Bliss and T. Lomo, J. Physiol. **32**, 331 (1973).
[3] M. C. Cross and P. C. Hohenberg, Rev. Mod. Phys. **65**, 851 (1993).
[4] G. Dupont and A. Goldbeter, Biophys. J. **67**, 2191 (1994).
[5] J. Sneyd, A. Charles, and M. Sanderson, Am. J. Physiol. **266**, C293 (1994).
[6] J. Sneyd and J. Sherratt, SIAM (Soc. Ind. Appl. Math.) J. Appl. Math. **57**, 73 (1997).
[7] J. Sneyd, S. Girard, and D. Clapham, Bull. Math. Biol. **55**, 315 (1993).
[8] A. Goldbeter, G. Dupont, and M. Berridge, Proc. Natl. Acad. Sci. U.S.A. **87**, 1461 (1990).
[9] J. Borghens, G. Dupont, and A. Goldbeter, Biophys. Chem. **66**, 25 (1997).
[10] G. Dupont, M. Berridge, and A. Goldbeter, Cell Calcium **12**, 73 (1991).
[11] G. Dupont and A. Goldbeter, BioEssays **14**, 485 (1992).
[12] G. Dupont and A. Goldbeter, Cell Calcium **14**, 311 (1993).
[13] G. Dupont and S. Swillens, Biophys. J. **71**, 1714 (1996).
[14] I. Bezprozvanny and B. Ehrlich, J. Membr. Biol. **145**, 205 (1995).
[15] I. Bezprozvanny, J. Watras, and B. Ehrlich, Nature (London) **351**, 751 (1991).
[16] M. Berridge, Nature (London) **361**, 315 (1993).
[17] M. Berridge, J. Physiol. **499**, 291 (1997).
[18] A. Bugrim, A. Zhabotinsky, and I. Epstein, Biophys. J. **73**, 2897 (1997).
[19] A. Bunde and S. Havlin, *Fractals and Disordered Systems* (Springer-Verlag, Berlin, 1991).